- Supporting Information -

Mechanical Properties and Molecular Adhesion Exhibited by Inorganic–Organic Composite Elastomers

Naoki Yamashita,[a] Ryohei Ikura,[a,b] Kenji Yamaoka,[a,b] Nobu Kato,[c] Masanao Kamei,[c] Kentaro Ogura,[c] Minoru Igarashi,[c] Hideo Nakagawa,[d] and Yoshinori Takashima[a,b,e]*

a. Department of Macromolecular Science, Graduate School of Science, Osaka University, 1-1 Machikaneyamacho, Toyonaka, Osaka 560-0043, Japan

b. Forefront Research Center, Graduate School of Science, Osaka University,1-1 Machikaneyamacho, Toyonaka, Osaka 560-0043, Japan

c. Shin-Estu Chemical Co., Ltd., Silicone-Electronics Materials Research Center, 1-10, Hitomi, Matsuida-machi, Annaka-shi, Gunma 379-0224, Japan

d. Shin-Etsu Chemical Co., Ltd., 4-1 Marunouchi, 1-chome, Chiyoda-ku, Tokyo 100-0005, Japan

e. Innovative Catalysis Science Division, Institute for Open and Transdisciplinary Research Initiatives, Osaka University, 1-1 Yamadaoka, Suita, Osaka 565-0871, Japan

Content

S1. Materials

Thiol-modified polydimethylsiloxane (PDMS-SH) was obtained from Shin-Etsu Chemical Co., Ltd. Allyl alcohol and ethyl acetate were purchased from FUJIFILM Wako Pure Chemical Corporation. 2-Hydroxy-2-methylpropiophenone (IRGACURE 1173) was purchased from Sigma–Aldrich Co. Ethyl acrylate (EA) was purchased from Nacalai Tesque, Inc. Phenylbis(2, 4, 6-trimethylbenzoil)phosphine oxide was purchased from Tokyo Chemical Industry Co., Ltd. Deuterated chloroform ($CDCl_3$) was purchased from Eurisotop. Triacetylated 6-acrylamido methylether-β-cyclodextrin (TAcβCDAAmMe) was purchased from Kyoeisha Chemical Co., Ltd. *N*-(1-adamantyl)acrylamide (AdAAm) was purchased from Yushiro Chemical Industry Co., Ltd.

S2. Measurements

Nuclear magnetic resonance (NMR) spectroscopy: ^{1}H NMR spectra were recorded at 400 MHz with a JEOL ECS-400 NMR spectrometer at 25 °C. ^{1}H-^{1}H nuclear Overhauser effect spectroscopy (NOESY) NMR spectra were recorded at 600 MHz with an Agilent VNS600 NMR spectrometer at 25 °C. Chemical shift values were referenced to the $CHCl_3$ value (δ = 7.26 ppm) for ^{1}H NMR.

Gel permeation chromatography (GPC): Number-average molecular weight (M_n), weight average molecular weight (M_w), and molecular weight distribution (M_w/M_n) were measured by GPC in THF at 40 °C with two columns (Tosoh TSK gel SuperHZM-N ×2). The molecular weights of the samples were calculated based on calibration curve got by polystyrene standards.

Tensile test: Tensile tests of the elastomers were performed using an Autograph AG-X plus (Shimadzu Co.) at a deformation rate of 1.0 and 0.1 mm/s. Rectangular test pieces (20 mm × 5 mm × 0.5 mm) were used for the tensile test. The toughness was calculated from the integral of the stress–strain curve. The Young's modulus was calculated from the initial slope of the stress–strain curve at a range of 1-6% strain.

Cyclic tensile test: Cyclic tensile tests were performed using an Autograph AG-X plus (Shimadzu Co.). Rectangular test pieces (20 mm × 5 mm × 0.5 mm) were continuously stretched and recovered without interval, where the maximum strains were set to 140%, 280%, 420%, 560%, 700%, 840%, and 980% with a deformation rate of 1 mm/s

Stress relaxation test: Stress relaxation tests were performed using an Autograph AG-X plus (Shimadzu Co.). The test pieces were stretched until 100%. Then, the strain was held, and the stress was recorded for 1000 seconds.

X-ray scattering measurements: The internal structures of the elastomers were determined by small-angle X-ray scattering (SAXS) measurements at the BL19B2 beam line in SPring-8, Nishi-harima, Japan. The power of the incident X-ray beams for BL19B2 was 18 keV. The sample-to-detector lengths for SAXS measurements was 3 m. The length of the scattering vector q in the SAXS measurements was 0.1-3 nm^{-1}, where $q = 4\pi\sin/\lambda$ (2θ and λ are the scattering angle and the wavelength, respectively).

Fourier transform infrared (FT-IR) spectroscopy: FT-IR spectra were acquired in ATR mode through diamond crystals with N_2 gas flow (JASCO FT/IR-410).

S3. Preparation of PDMS-CD

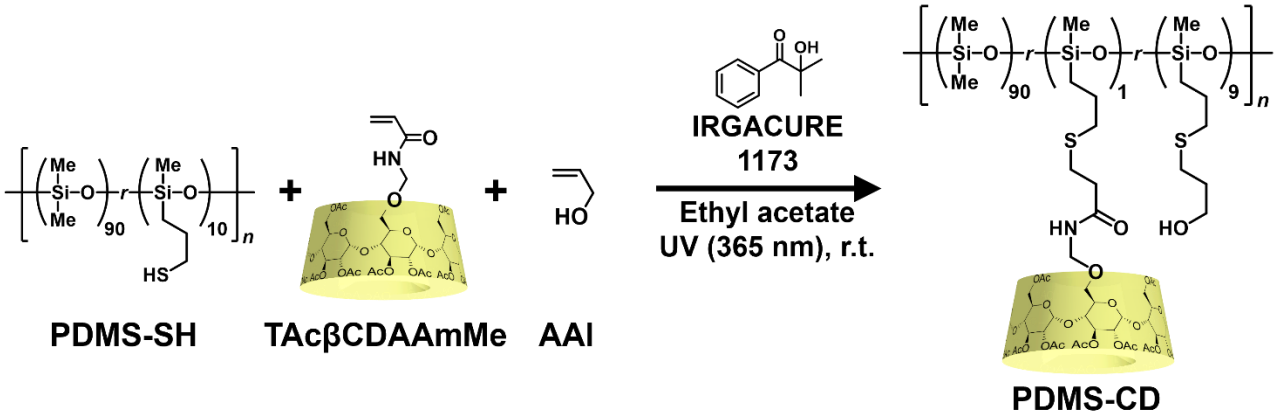

Scheme S1. Preparation of PDMS-CD.

PDMS-SH (4500 mg, SH group: 5.6 mmol, 10 eq.), TAcβCDAAmMe (1200 mg, 0.55 mmol, 1 eq.), allyl alcohol (290 mg, 5.0 mmol, 9 eq.), and IRGACURE 1173 (92 mg, 0.56 mmol, 1 eq.) were dissolved in ethyl acetate (20 mL). The solution was irradiated by UV light with a high-pressure Hg lamp (λ = 253 and 365 nm) for 2 hours.

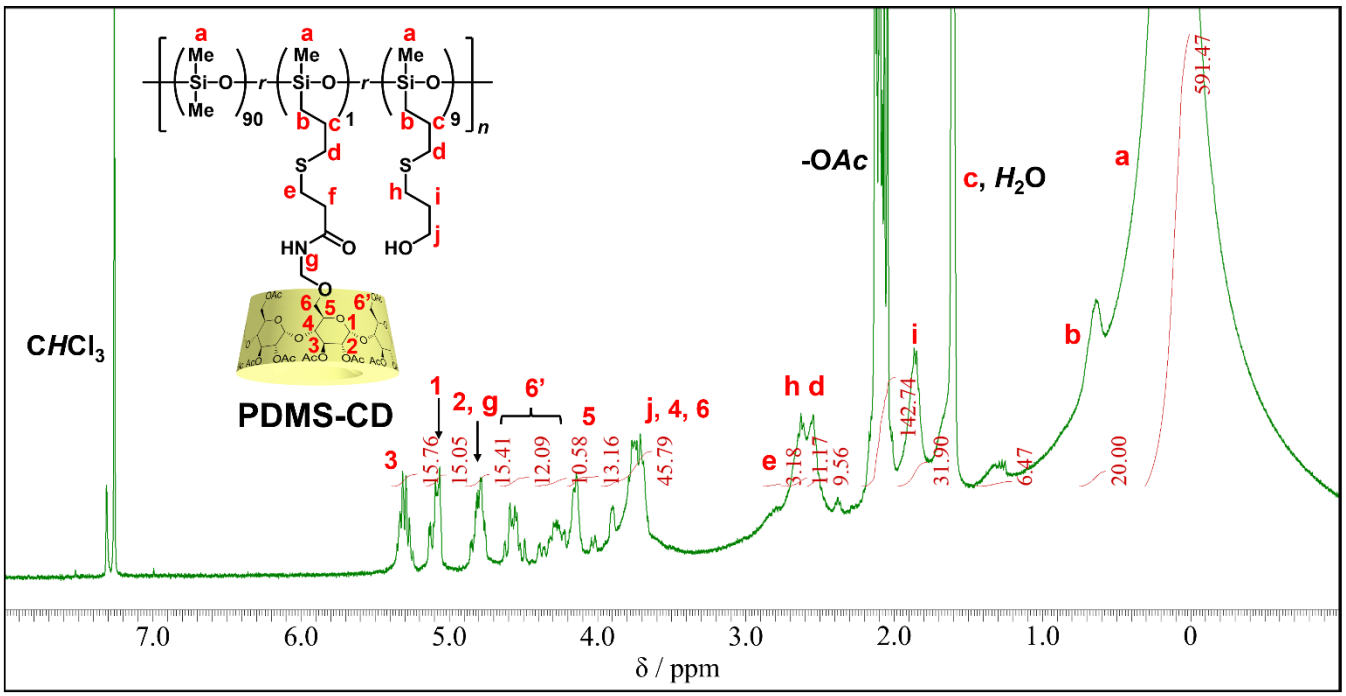

Figure S1. ^{1}H NMR spectrum of PDMS-CD ($CDCl_3$, 400 MHz, 25 °C).

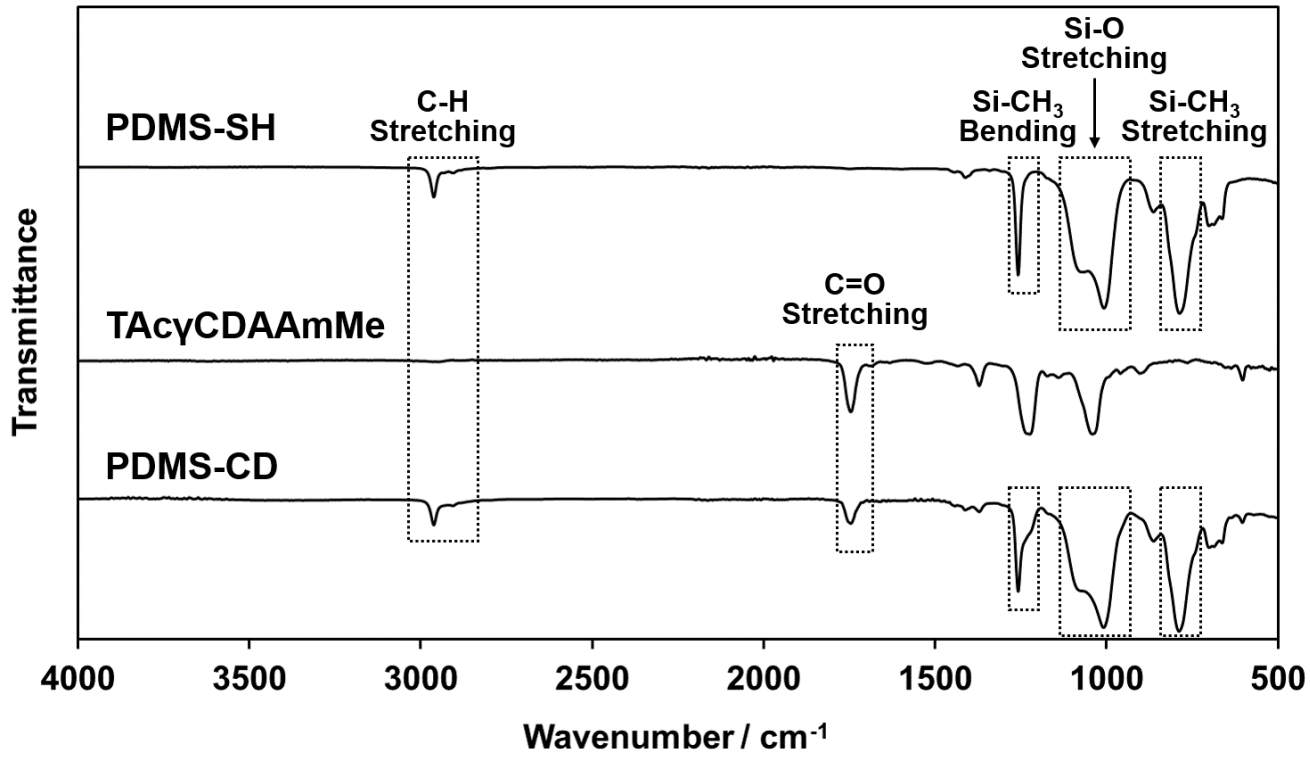

Figure S2. FT-IR spectra of PDMS-SH, TAcγCDAAmMe, and PDMS-CD.

S4. Preparation of PDMS-CD/P(EA-Ad) (*x*)

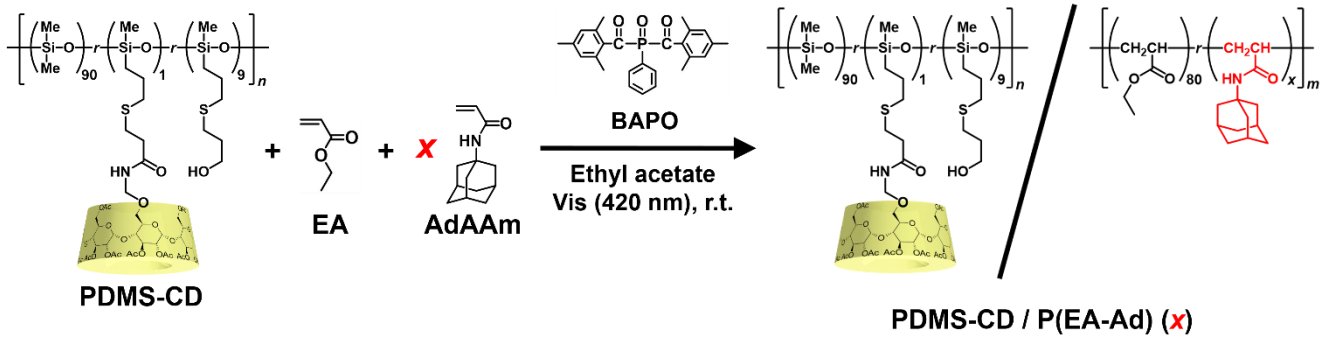

Scheme S2. Preparation of PDMS-CD/P(EA-Ad) (*x*).

EA, AdAAm, and BAPO were added to ethyl acetate solution of PDMS-CD (4800 mg, including 1200 mg of PDMS-CD). The solution was irradiated by visible light with a LED (λ = 420 nm) for 1 hour. The products were dried at r.t. for 24 hours and then at 80 ℃ in vacuum for 24 hours. Table S1 summarize amounts of reagents in the reactions.

Table S1. Amount of each reagent for PDMS-CD/P(EA-Ad) (*x*).

x /mol%	EA		AdAAm		BAPO	
	/mg	/mmol	/mg	/mmol	/mg	/mmol
1	900	9.0	23	0.11	19	0.045
2	900	9.0	46	0.22	19	0.045
5	900	9.0	120	0.56	19	0.045

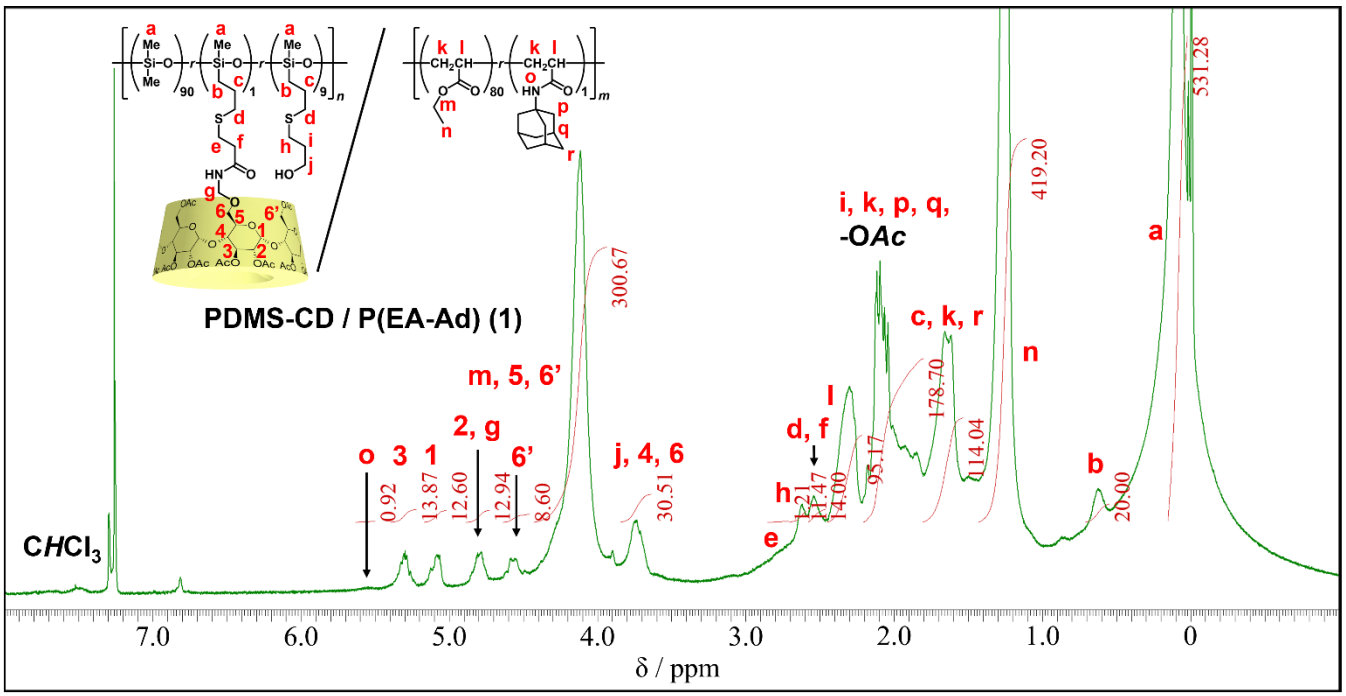

Figure S3. ^{1}H NMR spectrum of PDMS-CD/P(EA-Ad) (1) ($CDCl_3$, 400 MHz, 25 °C).

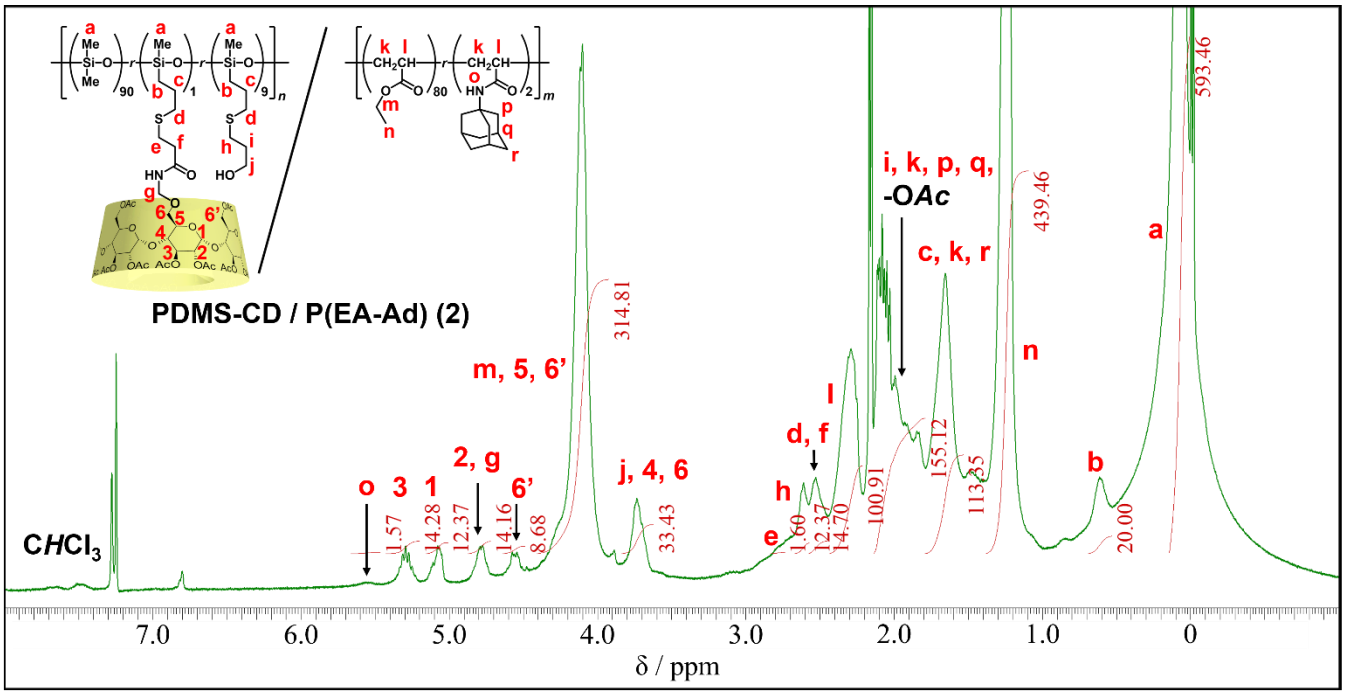

Figure S4. ^{1}H NMR spectrum of PDMS-CD/P(EA-Ad) (2) ($CDCl_3$, 400 MHz, 25 °C).

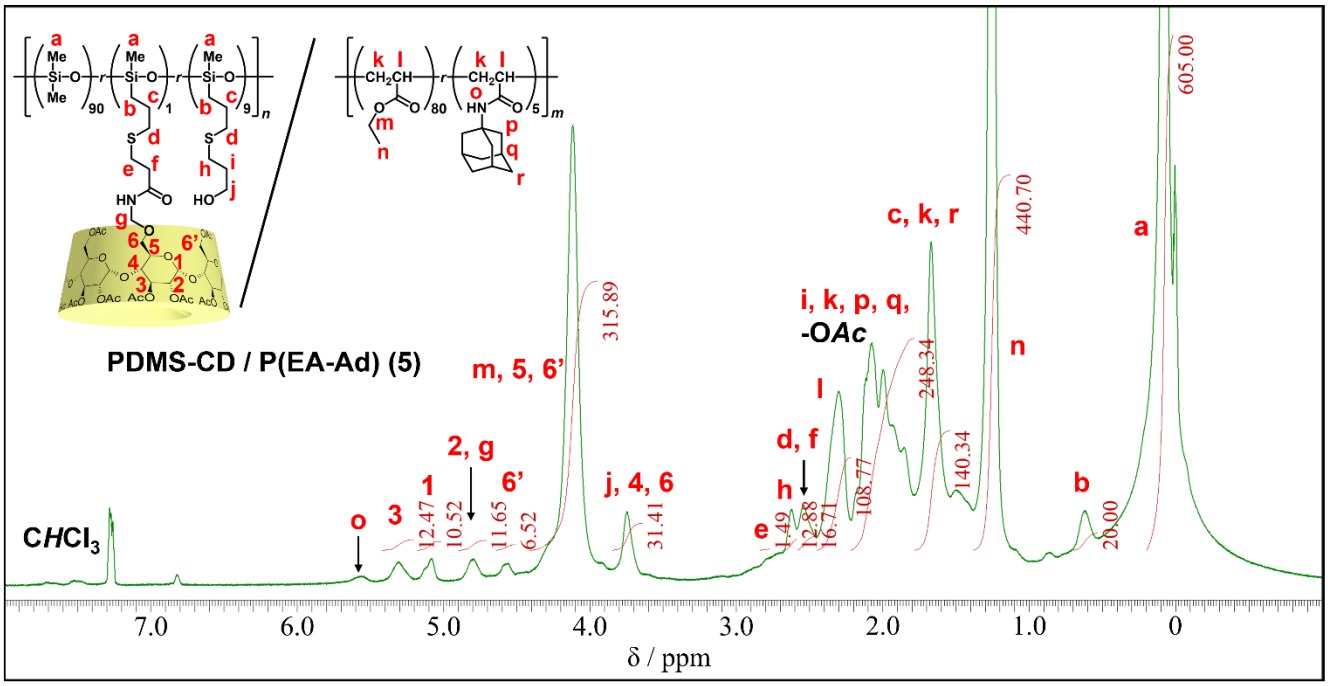

Figure S5. ^{1}H NMR spectrum of PDMS-CD/P(EA-Ad) (5) ($CDCl_3$, 400 MHz, 25 °C).

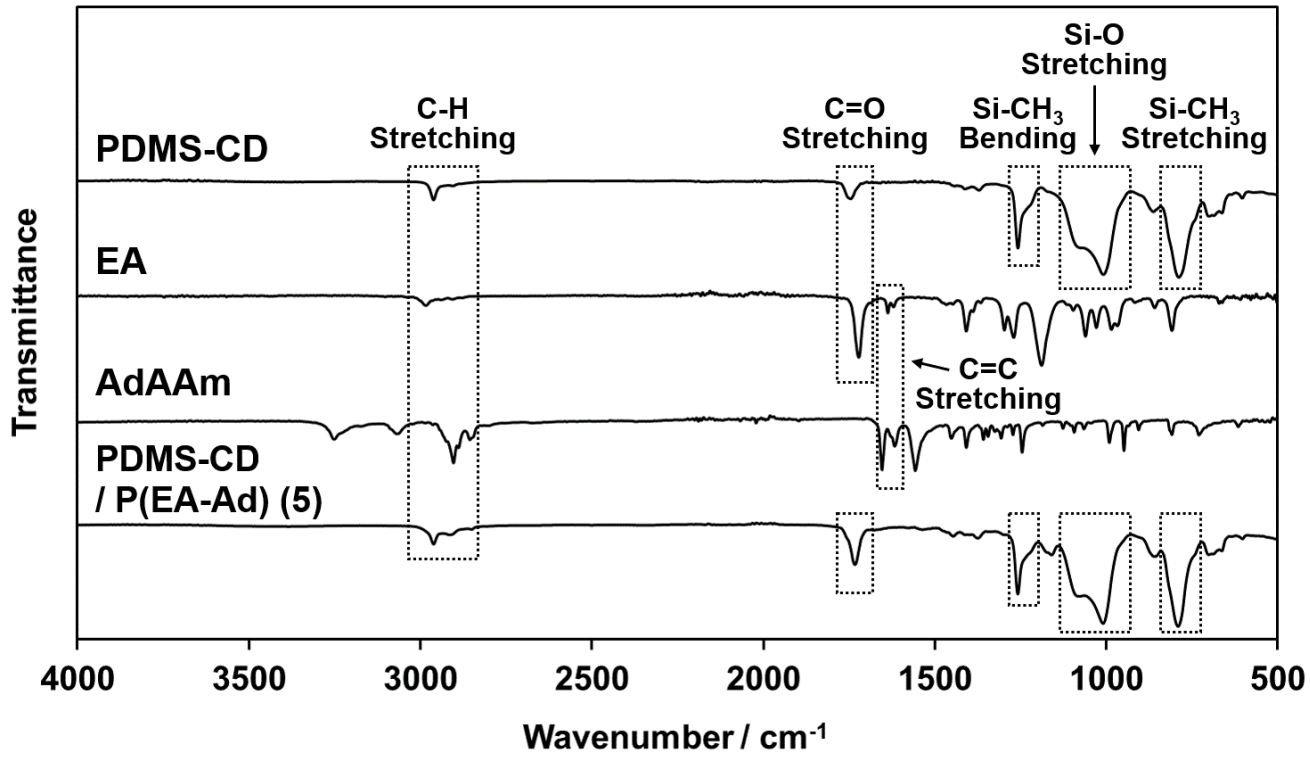

Figure S6. FT-IR spectra of PDMS-CD, EA, AdAAm, and PDMS-CD/P(EA-Ad) (5).

S5. Preparation of PDMS-CD/PEA

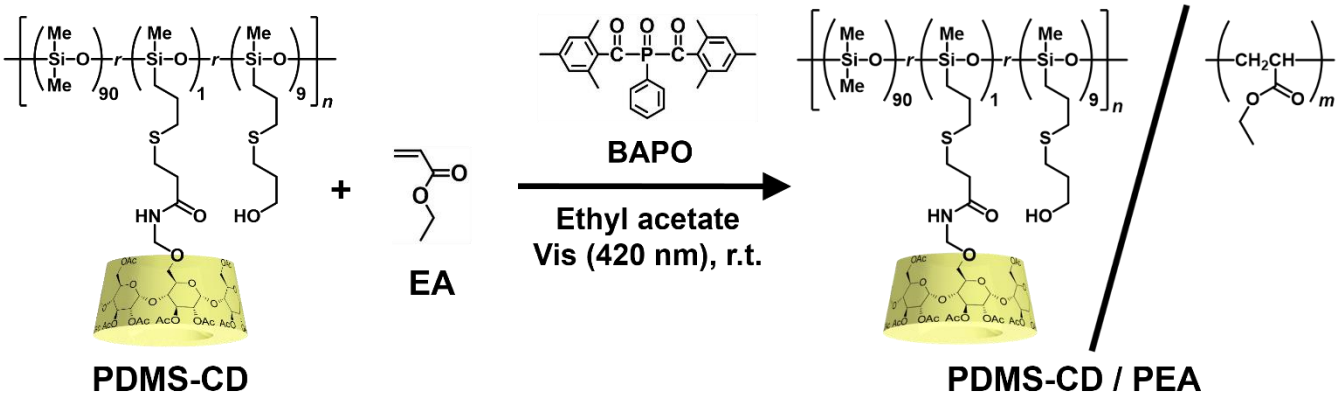

Scheme S3. Preparation of PDMS-CD/PEA.

EA (900 mg, 9.0 mmol) and BAPO (19 mg, 0.045 mmol) were added to ethyl acetate solution of PDMS-CD (4800 mg, including 1200 mg of PDMS-CD). The solution was irradiated by visible light with a LED (λ = 420 nm) for 1 hour. The products were dried at r.t. for 24 hours and then at 80 ℃ in vacuum for 24 hours.

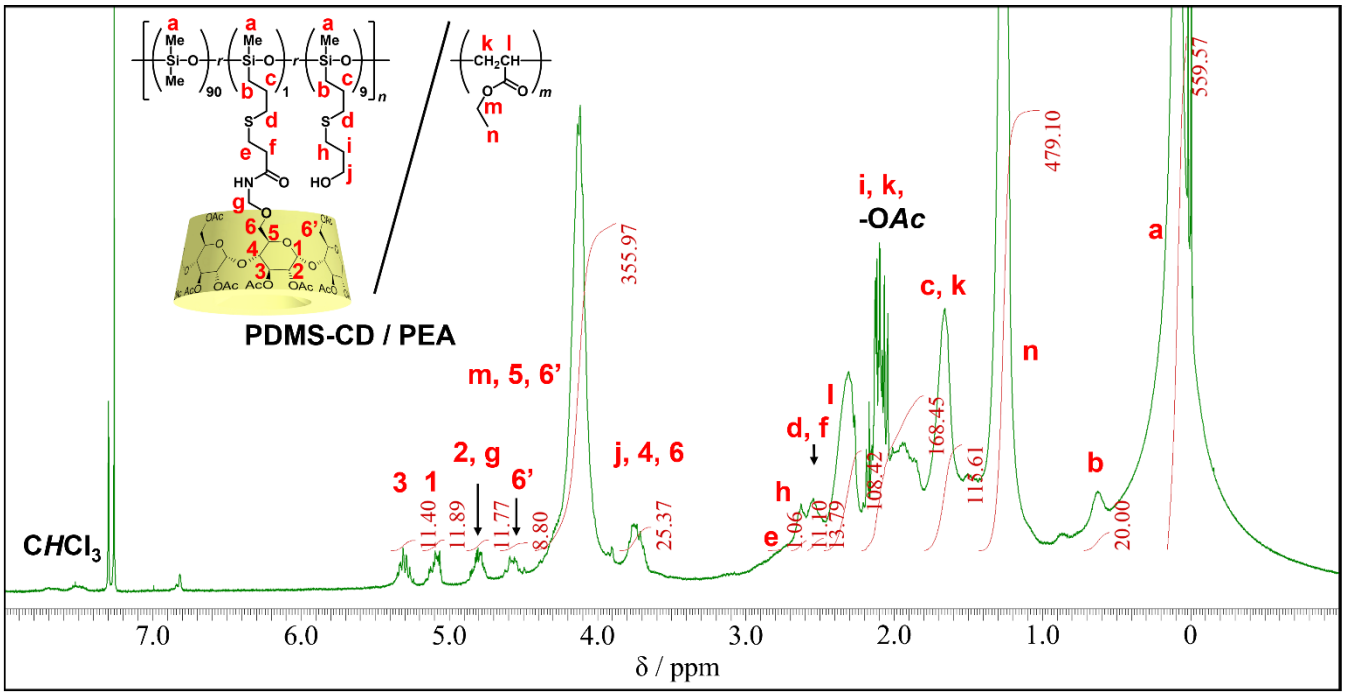

Figure S7. ^{1}H NMR spectrum of PDMS-CD/PEA ($CDCl_3$, 400 MHz, 25 ℃).

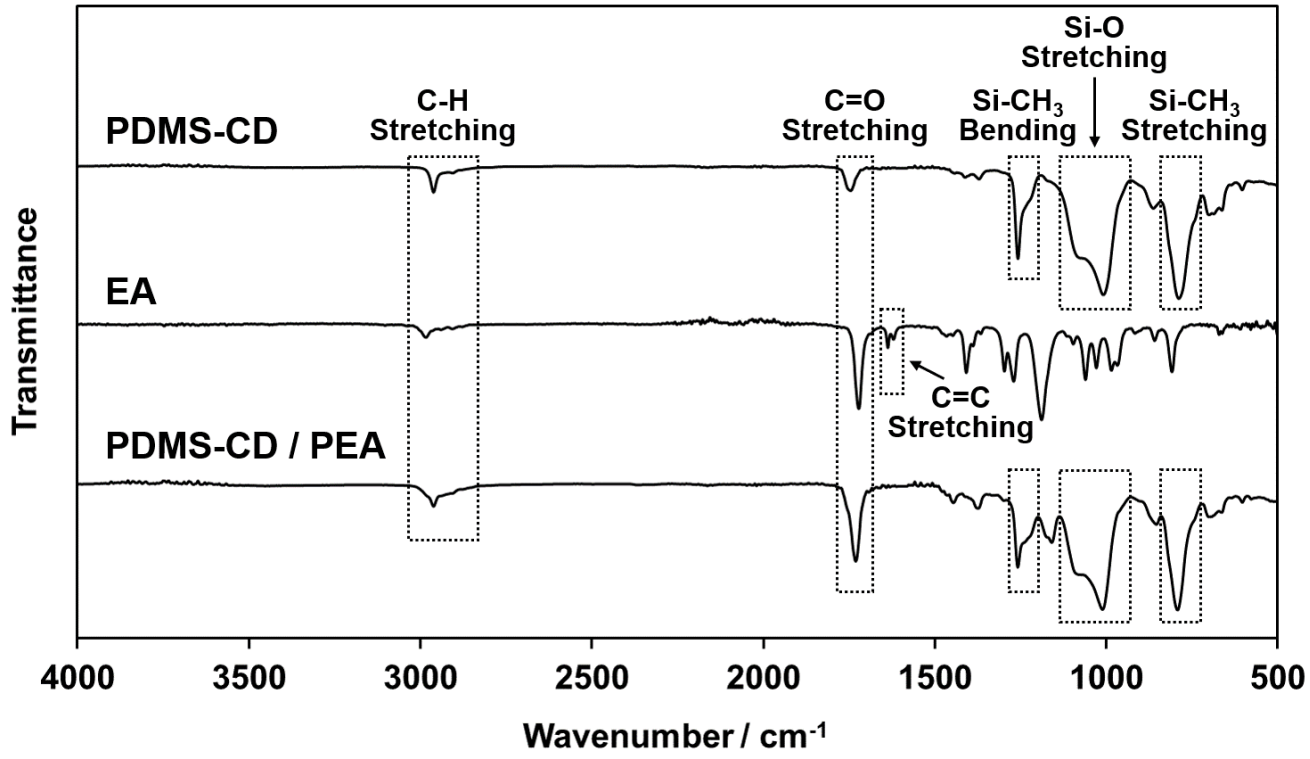

Figure S8. FT-IR spectra of PDMS-CD, EA, and PDMS-CD/PEA.

S6. Preparation of PDMS/P(EA-Ad) (5)

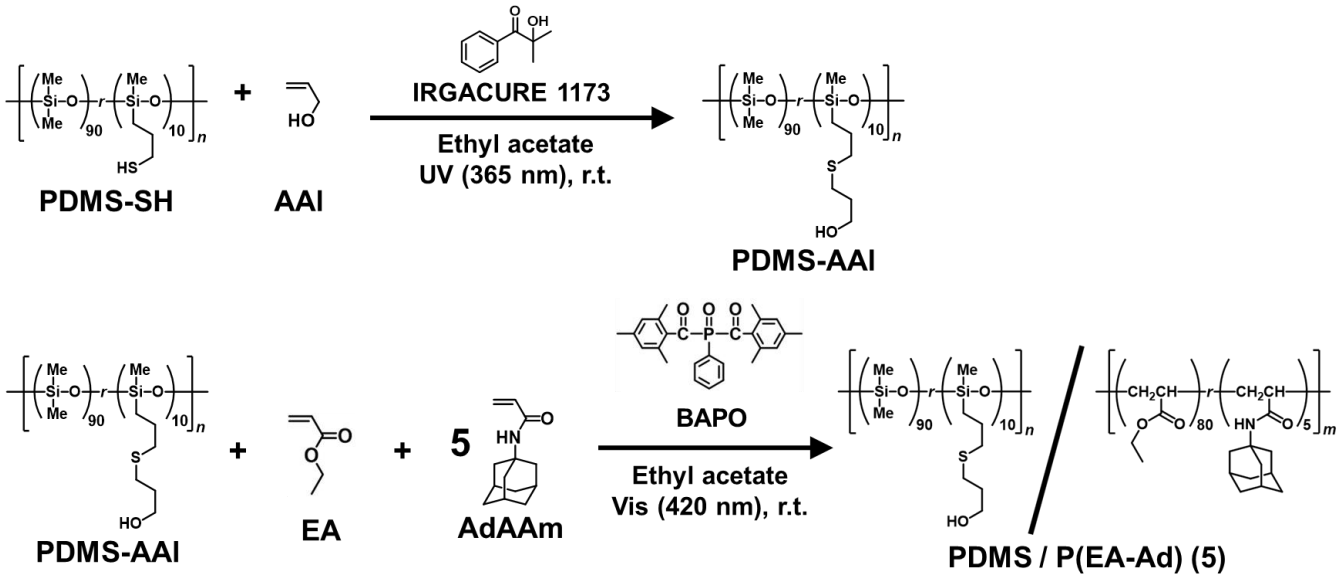

Scheme S4. Preparation of PDMS/P(EA-Ad) (5).

PDMS-SH (4500 mg, SH group: 5.6 mmol, 10 eq.), allyl alcohol (330 mg, 5.7 mmol, 10 eq.), and IRGACURE 1173 (92 mg, 0.56 mmol, 1 eq.) were dissolved in ethyl acetate (20 mL). The solution was irradiated by UV light with a high-pressure Hg lamp (the dominant wavelength, λ = 253 and 365 nm) for 2 hours. The exposure enargy is 2.05 mW/cm^2 at λ = 365 nm. EA (900 mg, 9.0 mmol), AdAAm (120 mg, 0.56 mmol), and BAPO (19 mg, 0.045 mmol) were added to obtained ethyl acetate solution of PDMS-AAl (4600 mg, including 960 mg of PDMS-AAl). The solution was irradiated by visible light with a LED (λ = 420 nm) for 1 hour. The products were dried at r.t. for 24 hours and then at 80 ℃ in vacuum for 24 hours.

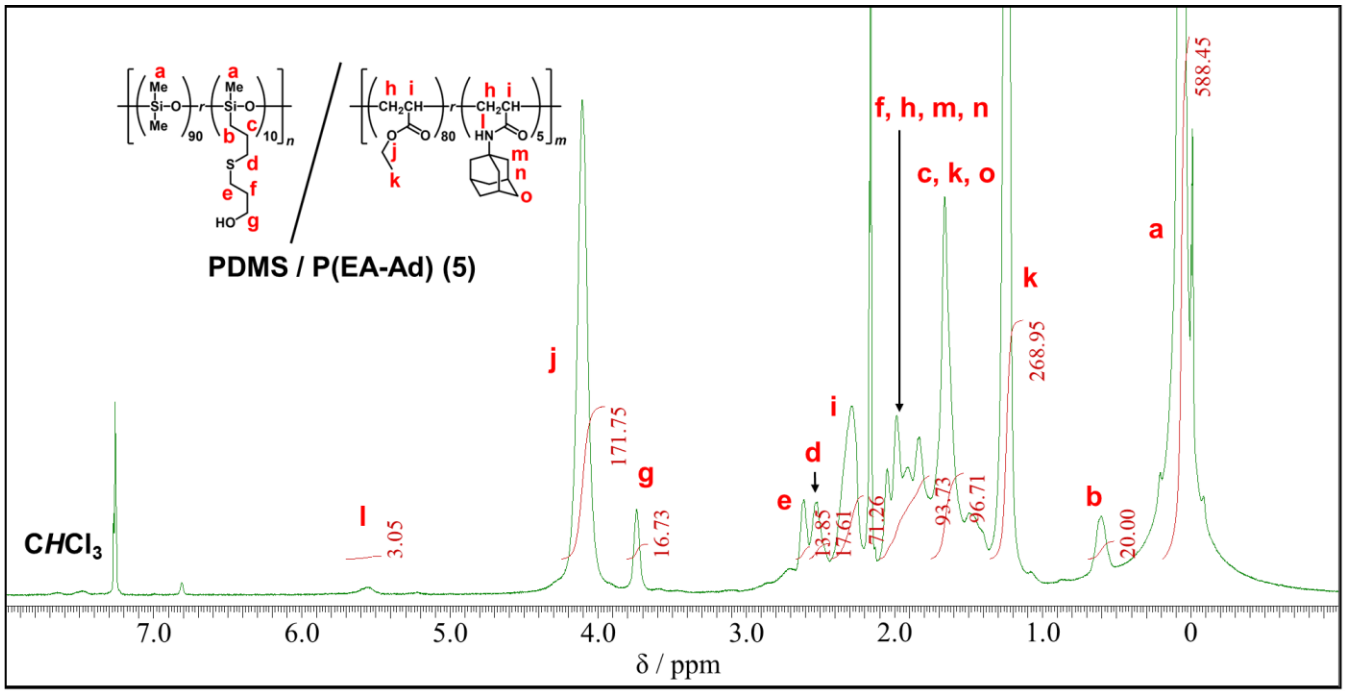

Figure S9. ^{1}H NMR spectrum of PDMS/P(EA-Ad) (5) ($CDCl_3$, 400 MHz, 25 ℃).

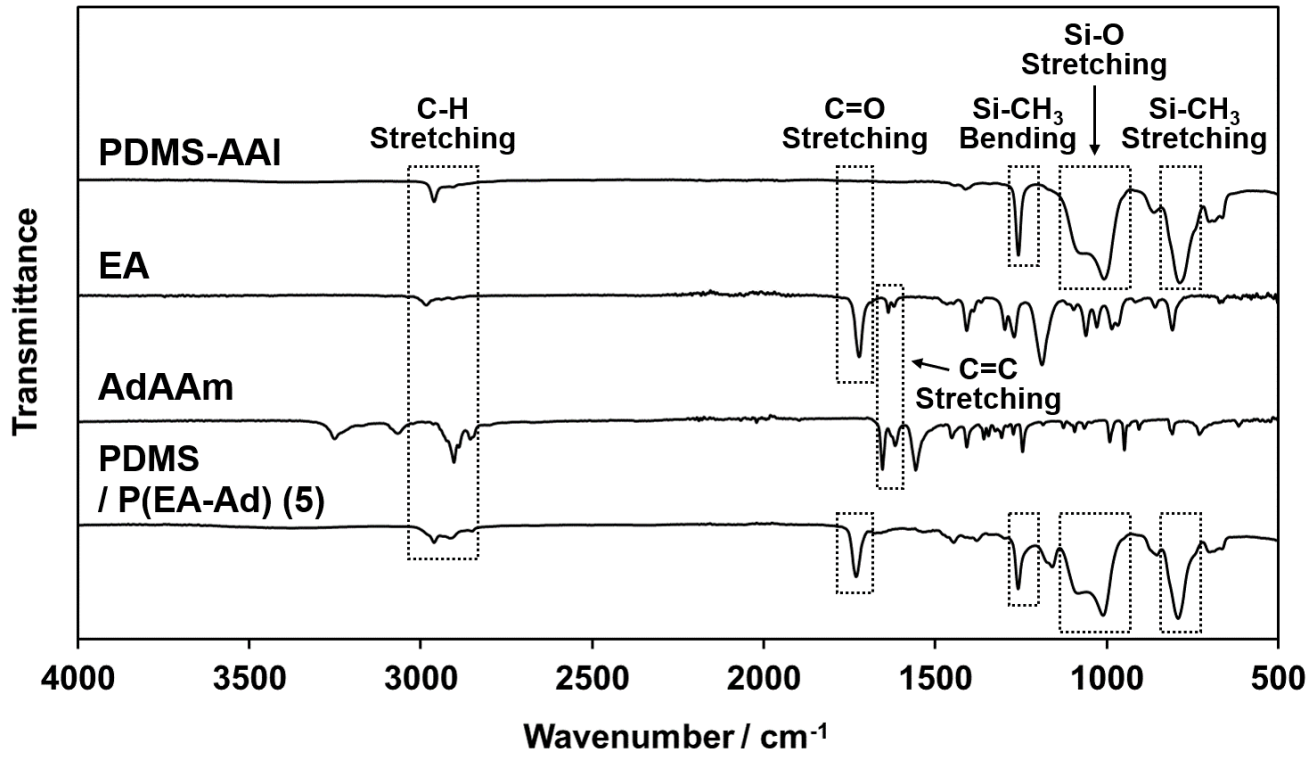

Figure S10. FT-IR spectra of PDMS-SH, EA, AdAAm, and PDMS/P(EA-Ad) (5).

S7. Preparation of PDMS/PEA

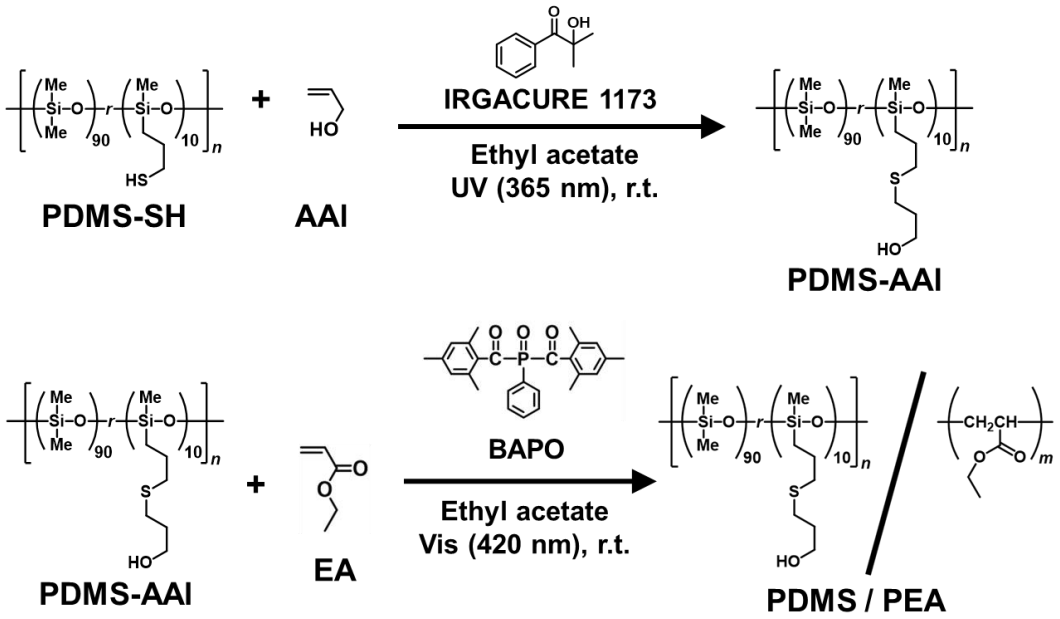

Scheme S5. Preparation of PDMS/PEA.

PDMS-SH (4500 mg, SH group: 5.6 mmol, 10 eq.), allyl alcohol (330 mg, 5.7 mmol, 10 eq.), and IRGACURE 1173 (92 mg, 0.56 mmol, 1 eq.) were dissolved in ethyl acetate (20 mL). The solution was irradiated by UV light with a high-pressure Hg lamp (the dominant wavelength, λ = 253 and 365 nm) for 2 hours. The exposure enargy is 2.05 mW/cm^2 at λ = 365 nm. EA (900 mg, 9.0 mmol) and BAPO (19 mg, 0.045 mmol) were added to obtained ethyl acetate solution of PDMS-AAl (4600 mg, including 960 mg of PDMS-AAl). The solution was irradiated by visible light with a LED (λ = 420 nm) for 1 hour. The products were dried at r.t. for 24 hours and then at 80 ℃ in vacuum for 24 hours.

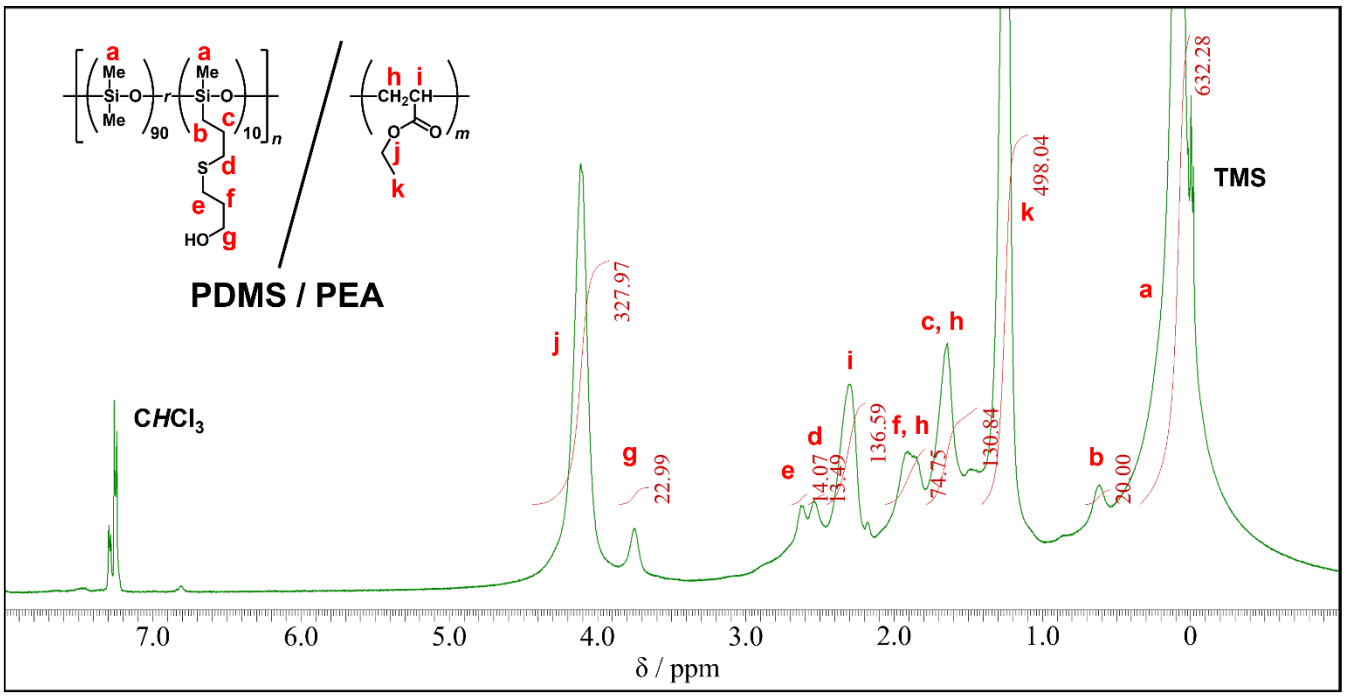

Figure S11. ^{1}H NMR spectrum of PDMS/PEA ($CDCl_3$, 400 MHz, 25 °C).

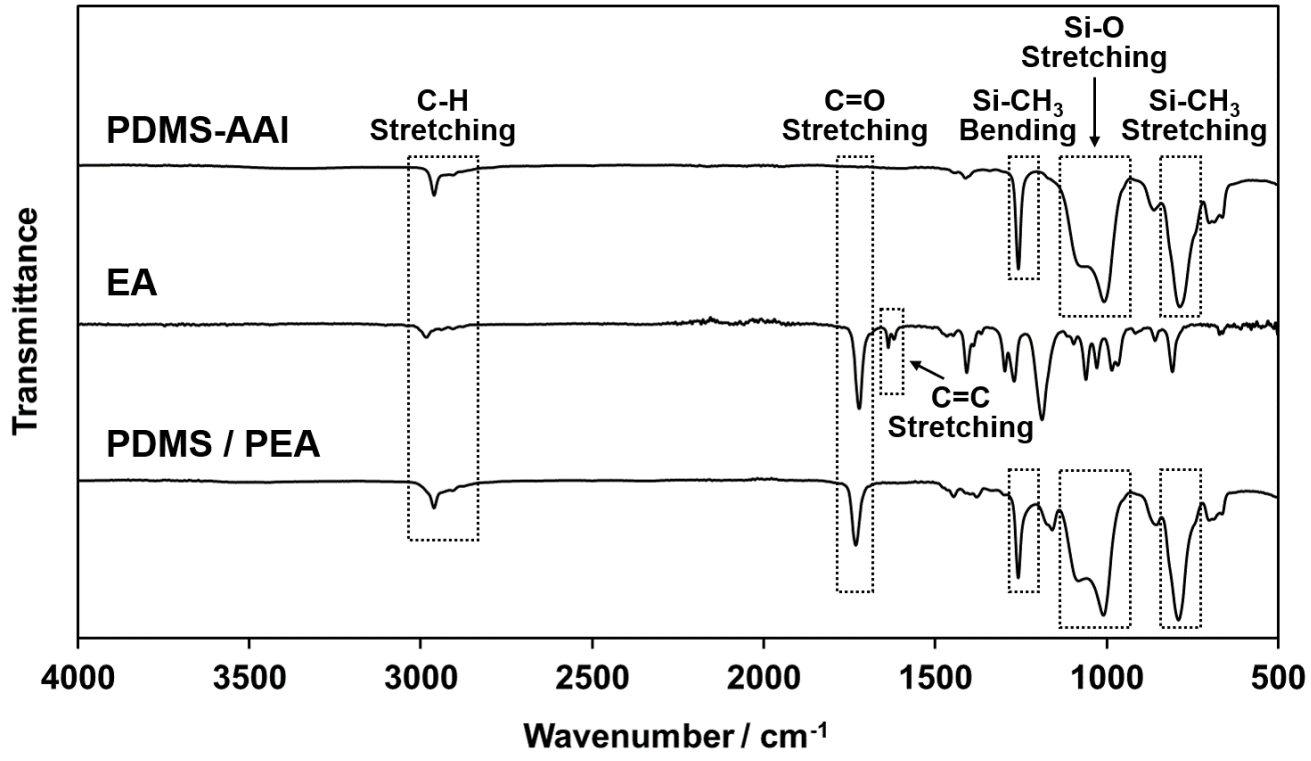

Figure S12. FT-IR spectra of PDMS-SH, EA, and PDMS/PEA.

S8. Investigation of molecular weight by GPC

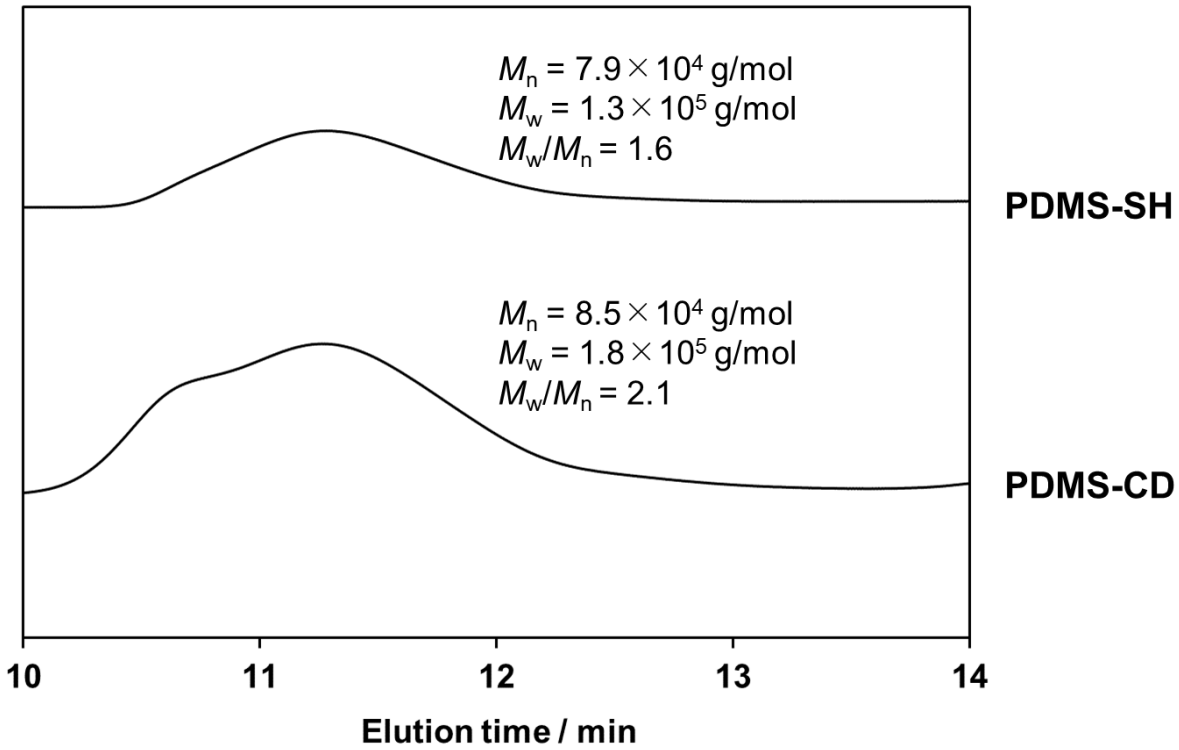

Figure S13. GPC chart of PDMS-SH and PDMS-CD.

S9. Confirmation of inclusion complex formation by NOESY NMR

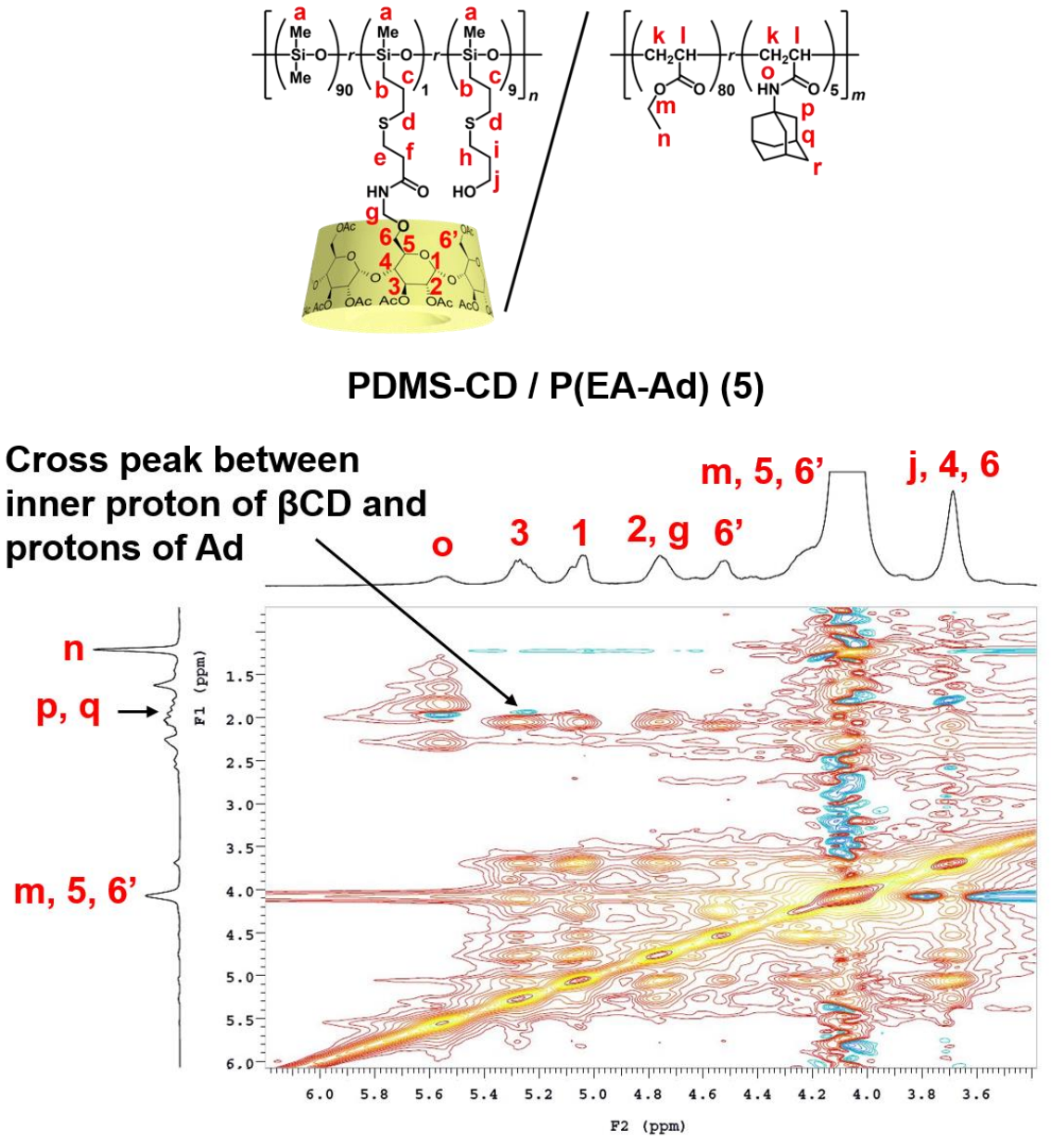

Figure S14. 2D NOESY NMR spectrum of PDMS-CD/P(EA-Ad) (5) ($CDCl_3$, 600 MHz, 25 °C, mixing time τ = 1000 ms).

S10. Investigation of deformation behaviors in cyclic tensile test

We investigated the effect of the reversible cross-links with cyclic tensile tests of PDMS-CD/P(EA-Ad) (5). The analysis revealed three distinct modes of molecular motion in PDMS-CD/P(EA-Ad) (5): phase separation, exchange of reversible cross-links, and extension of polymer chains. The detailed discussion is as follows:

(i) Phase separation of PEA and PDMS domains in the low strain region

The stretching curves from 2nd cycle exhibit significantly lower stress compared to the 1st cycle, indicating inadequate recovery of mechanical properties due to substantial structural changes caused by stress-induced phase separation. Previous research on composites with movable cross-links connecting dissimilar polymers also showed stress-induced phase separation at low strains (0–120%) in SAXS profiles of composite elastomers under tensile deformation[1]. Therefore, the upward convex shape of the stress-strain curve for PDMS-CD/P(EA-Ad) (5) at low strains is attributed to stress-induced phase separation.

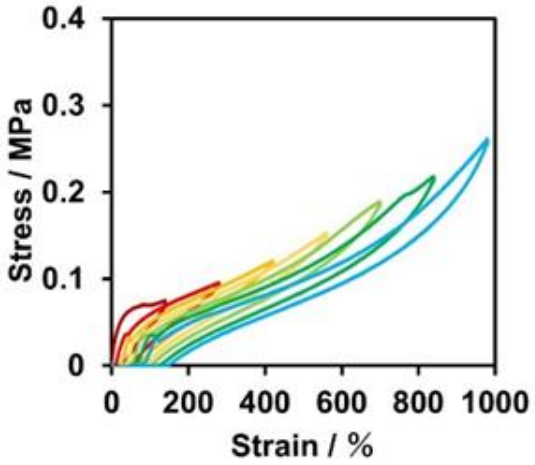

Figure S15. A cyclic tensile test for PDMS-CD/P(EA-Ad) (5).

(ii) Exchange of reversible cross-links in the middle strain region

In the 2nd through 5th cycles, the decrease in the stress of stretching curves is moderate, indicating the effective recovery of the mechanical properties due to reformation and exchanging of the host-guest complex. Thus, the S-shaped curve with a wide range of small slopes in middle strain region can be attributed to the stress relaxation resulting from the exchange of reversible cross-links.

(iii) Extending polymer chains in the high strain region

The downward convex stress-strain curves at high strain is characteristic of stress-hardening due to the extension of polymer chains. In the 5th through 7th cycles, the significant decrease in the stress of stretching curves indicates the inadequate recovery during this timescale.

S11. Investigation of the network structure by swelling tests

To characterize the network structures, we conducted swelling tests using chloroform as the swelling solvent. The polymers were immersed in excess chloroform for two days. The swelling ratio (Q) was determined by the following equation:

$$\text{Swelling ratio } (Q) = \frac{W - W_0}{W_0} \times 100\% \quad \text{(S1)}$$

where W is the weight of the swollen polymer and W_0 is the initial weight of the polymer before swelling.

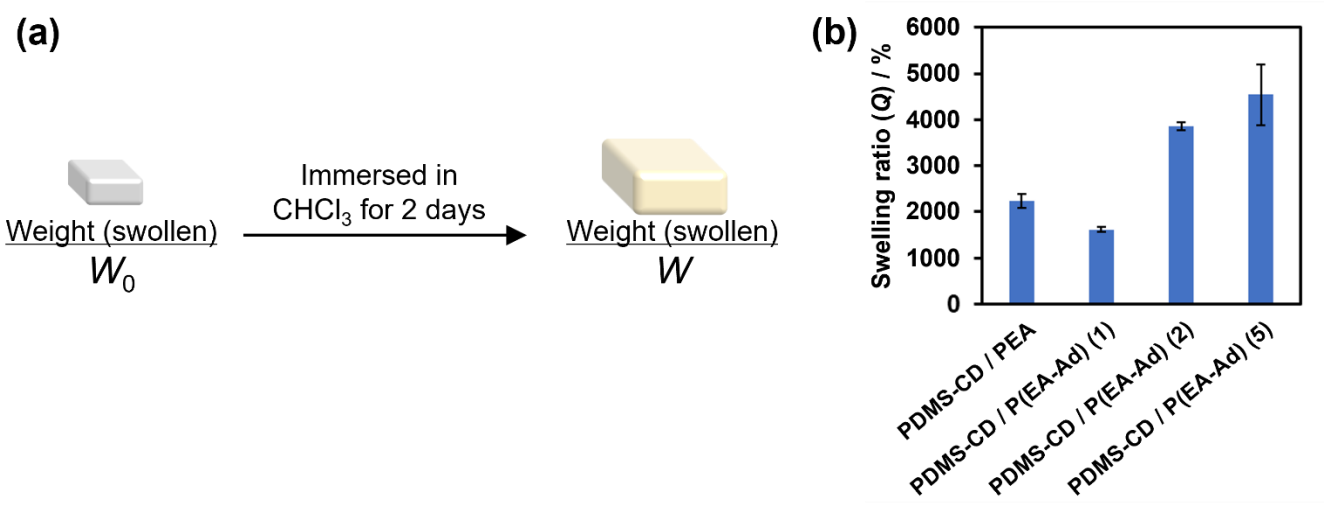

Figure S16. (a) Experimental procedure of the swelling test. **(b)** Swelling ratios of PDMS-CD/PEA and PDMS-CD/P(EA-Ad) (x) (x = 1, 2, and 5).

S12. Evaluation of the stress dispersion property by stress relaxation tests

Curve fitting was carried out on the obtained stress σ versus relaxation time t curves using the Kohlrausch–Williams–Watts models, as described by the following equation.

$$\sigma = \sigma_r \exp\left\{-\left(\frac{t}{\tau}\right)^{\beta}\right\} + \sigma_\infty \quad \text{(S2)}$$

In the above equation, σ_r is the relaxable stress, σ_∞ is the residual stress, τ is the time constant, and β is the stretching exponent.

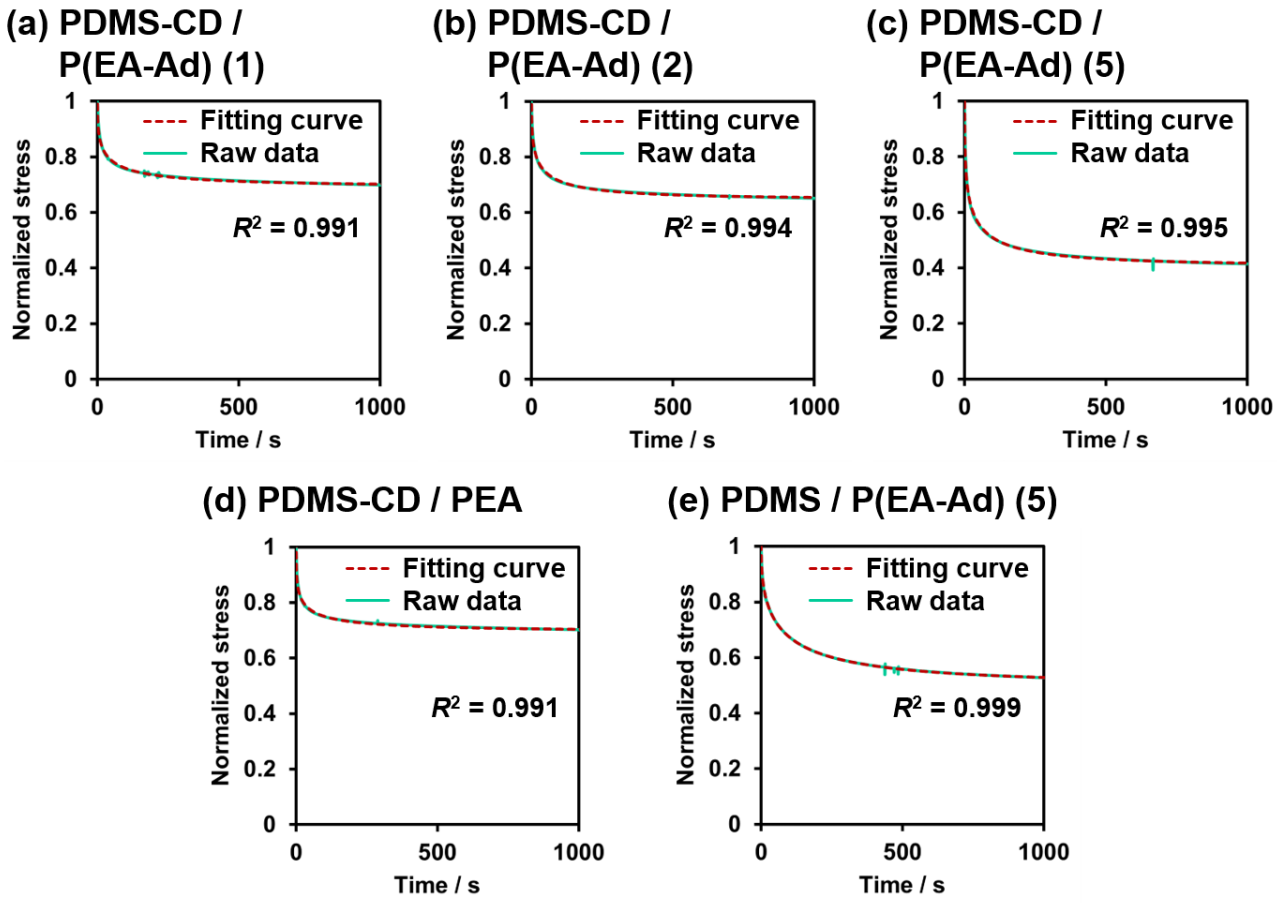

Figure S17. Stress relaxation curves of PDMS-CD/P(EA-Ad) (x) when x = **(a)** 1, **(b)** 2, **(c)** 5, **(d)** PDMS-CD/PEA, and **(e)** PDMS/P(EA-Ad) (5) with fitting curves (raw data: cyan solid line, fitting curves: brown dashed line).

Table S2. Fitting parameters obtained for PDMS-CD/P(EA-Ad) (*x*), PDMS-CD/PEA, and PDMS/P(EA-Ad) (5) by using the KWW models.

	Relaxable component			Residual component
	σ_r	τ / s	β	σ_∞
PDMS-CD / P(EA-Ad) (1)	0.33	17	0.33	0.67
PDMS-CD / P(EA-Ad) (2)	0.37	21	0.37	0.63
PDMS-CD / P(EA-Ad) (5)	0.61	19	0.36	0.39
PDMS-CD / PEA	0.32	16	0.33	0.68
PDMS / P(EA-Ad) (5)	0.50	81	0.45	0.50

S13. Tensile test at different tensile rates

The tensile tests of PDMS-CD/PEA and PDMS-CD/P(EA-Ad) (*x*) (*x* = 1, 2, and 5) were performed at 0.1 and 1.0 mm/s. The tensile test of all composites at 0.1 mm/s show decrease in toughness. Too slow tensile speed decreases the elasticity of reversible cross-links connecting the PDMS and PEA domains, impairing the cooperative deformation of these domains to decrease the toughness. In our previous work[R1], composites with movable cross-links also exhibited reduced toughness under slower tensile deformation. The decreases in the elasticity of reversible cross-links also leads to the reduction in Young's modulus. PDMS-CD/P(EA-Ad) (5) shows the largest decrease in the Young's modulus. PDMS-CD/PEA and PDMS-CD/P(EA-Ad) (*x*) (*x* = 1, 2, and 5) show similar time constant (τ), which contributes to the similar dependency of mechanical properties on tensile speed.

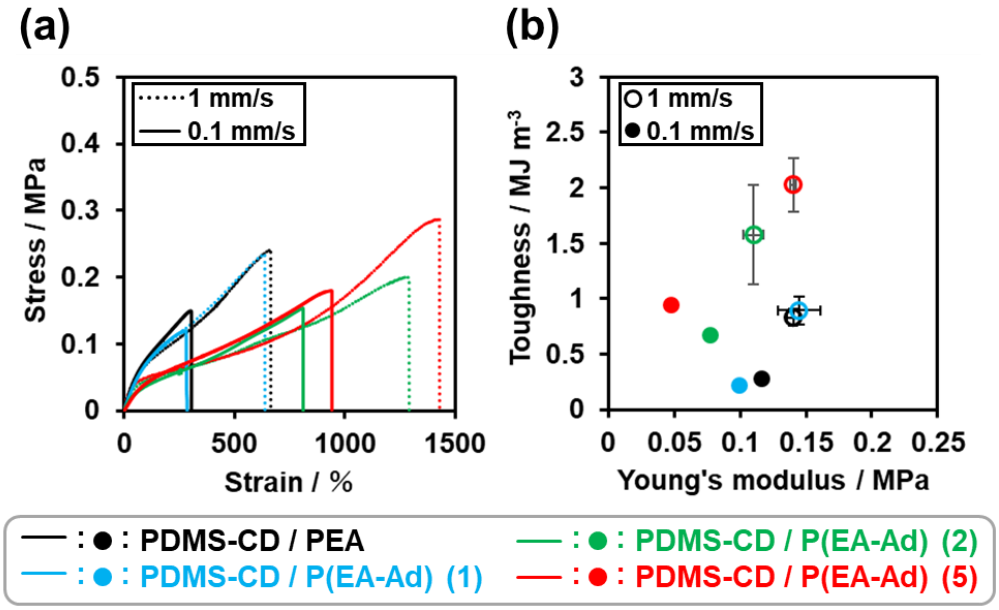

Figure S18. (a) Stress–strain curves and **(b)** plots of the toughness and Young's modulus values of PDMS-CD/PEA and PDMS-CD/P(EA-Ad) (*x*) (*x* = 1, 2, and 5) with tensile rate of 1 or 0.1 mm/s.

S14. References

[1]. R. Ikura, S. Murayama, J. Park, Y. Ikemoto, M. Osaki, H. Yamaguchi, A. Harada, G. Matsuba and Y. Takashima *Molecular Systems Design & Engineering* 2022, **7**, 733-745.